



ELSEVIER

15 May 1997

OPTICS  
COMMUNICATIONS

Optics Communications 138 (1997) 242–248

Full length article

# Four-wave light scattering by polaritons in $\text{LiNbO}_3$

G.Kh. Kitaeva<sup>\*</sup>, A.A. Mikhailovsky, P.S. Losevsky, A.N. Penin*Department of Physics, Moscow State University, Moscow 119899, Russia*

Received 17 September 1996; accepted 18 December 1996

## Abstract

We report the results of the experimental study of the four-wave polariton scattering in  $\text{LiNbO}_3$ . Different types of scattering processes and their mutual influence are considered. Analyzing the angular dependences of the scattering intensity, we show that the cascade coherent type of interaction is predominant in  $\text{LiNbO}_3$ . Perspectives of the measurement of refractive indexes and absorption coefficients at polariton frequencies are discussed.

PACS: 42.65.Dr; 42.65.-k; 63.20.-e

## 1. Introduction

Spectroscopy of light scattering by polaritons is an extremely sensitive method for investigation of relatively small variations of the medium properties. In contrast to the Raman spectroscopy, it enables one to measure oscillator strengths and dispersion dependences both for the real and imaginary parts of the dielectric function near phonon resonances. Such effects as variation of the doping agent concentration, spatial inhomogeneity, low-dimensional effects, etc., do not often influence Raman spectra, though polariton state parameters change sufficiently. Dielectric properties of various media in the vicinity of the optical phonon frequencies as well as phonon oscillator strengths can be measured also by fitting the infrared reflectivity spectra. But in the case of scattering spectroscopy, all measurements of the scattered light intensity can be done in the visible range by a proper selection of the pump frequency. This enables one to take advantage of the visible radiation detecting technique. Besides, in the scattering spectroscopy surface and bulk effects can be easily separated.

The phenomenon of spontaneous three-wave scattering by polaritons is successfully employed for investigating the properties of crystalline noncentrosymmetric media

[1,2]. Dispersion dependences of the real and imaginary parts of the dielectric constant are determined by measuring the two-dimensional frequency-angular distribution of the scattered light intensity in the scheme of near-forward Raman scattering. When the shift between polariton and phonon frequencies is large in comparison with the phonon damping constant, scattering occurs due to the second-order optical susceptibility only. In this case, it is also called spontaneous parametric scattering [3]. For scattering on the upper polariton branch, it is known as spontaneous parametric down-conversion, a source of quantum noise in optical parametric oscillators [3,4]. In the vicinity of a phonon resonance, there is additional contribution to the scattering intensity from the Raman scattering tensor. However, the implementation of the spontaneous three-wave scattering by polaritons is often limited because of the low intensity of the scattered radiation. It makes the investigation of microscopic objects and media with small values of the quadratic nonlinear susceptibility  $\chi^{(2)}$  extremely difficult. One can solve this problem using the methods of four-wave mixing active polariton spectroscopy.

The first works in this area were started in the late 60s [5] and are carried out up to now [6]. The processes of four-wave mixing were considered both for the case of a centrosymmetric medium [7] and the case of a noncentrosymmetric one [5,8–12]. Most of the works were dedicated to the analysis of the interference of direct and

<sup>\*</sup> Corresponding author. Chair of Quantum Radiophysics.  
E-mail: postmast@spr.phys.msu.su.

cascade four-wave mixing processes and the investigation of cubic nonlinear susceptibility  $\chi^{(3)}$  dispersion. The goals of our work were to examine the features of the four-wave mixing polariton scattering processes and to propose the optimal experimental setup enabling us to measure the polariton dispersion law  $\omega(\mathbf{k})$ , the real  $\epsilon'(\omega)$  and the imaginary  $\epsilon''(\omega)$  parts of the dielectric function.

## 2. Conditions of the experiment

Four-wave mixing scattering was studied in Mg-doped lithium niobate crystals  $\text{LiNbO}_3:\text{Mg}$  with different mass concentration of the doping agent (0.68% and 0.79%). The crystals were grown from approximately congruent melt. The dispersion law of the polariton was measured beforehand by means of three-wave scattering spectra (for comparison with the data obtained by the four-wave method). The data on the refractive index in the visible and near IR region were taken from Ref. [13] for the sample with Mg mass concentration of 0.79%. For the sample with Mg mass concentration of 0.68%, the data were calculated taking into account the results of Ref. [13] for doped crystals and [14] for pure congruent  $\text{LiNbO}_3$ .

We implemented the most general scheme of the Stokes four-wave interaction (see Fig. 1). It is similar to the scheme proposed in Ref. [5], but instead of the anti-Stokes interaction, the Stokes one is considered. In this case, all pumping beams must have different frequencies. The use of the Stokes scheme enabled us to observe three-wave scattering by means of the same set-up when the exciting pumping beams were switched off. Pumping waves with the frequencies  $\omega_1$  and  $\omega_2$  located in the near IR region (“exciting” waves) excited the polariton state with fre-

quency corresponding to the frequency phase matching condition:

$$\omega_1 - \omega_2 = \omega_p, \quad (1)$$

$\omega_p$  is the frequency of the polariton state. We used IR beams for exciting polariton levels because it prevented the signal detector from registering parasite light of the exciting beams or any kind of luminescence caused by them. The cascade scattering process has the highest efficiency if the spatial phase matching condition for the wavevectors  $\mathbf{k}_i$  ( $i = 1, 2, p$ ) is satisfied:

$$\tau \equiv \mathbf{k}_1 - \mathbf{k}_2 - \mathbf{k}_p = 0. \quad (2)$$

The exciting waves were generated by a YAG: $\text{Nd}^{+3}$ -laser and a tunable  $\text{LiF}:F_2^-$ -laser with repetition rate of 1–33 Hz, pulse duration of about 20 ns, and with wavelengths  $\lambda_1 = 1.064 \mu\text{m}$  and  $\lambda_2$ , tunable in the spectral range 1.08–1.22  $\mu\text{m}$ , respectively. Radiation of the YAG: $\text{Nd}^{+3}$ -laser second harmonic with wavelength  $\lambda_L = 532 \text{ nm}$  was used as the third pumping beam – the “probe” one. The Stokes component of the scattered radiation was detected at the frequency

$$\omega_4 = \omega_3 - \omega_p = \omega_3 - (\omega_1 - \omega_2) \quad (3)$$

(hereafter the index 3 denotes the parameters of the probe wave and the index 4 denotes the parameters of the signal one, detected at the output of the medium). Note that at the same frequency there is Stokes three-wave spontaneous scattering of the probe pumping wave with frequency  $\omega_3$ . Both the direct and the cascade four-wave processes are most effective if they satisfy the common spatial phase matching condition:

$$\Delta \mathbf{k} = \mathbf{k}_4 - \mathbf{k}_3 + \mathbf{k}_1 - \mathbf{k}_2 = 0. \quad (4)$$

If the phase matching condition (2) is also satisfied, then

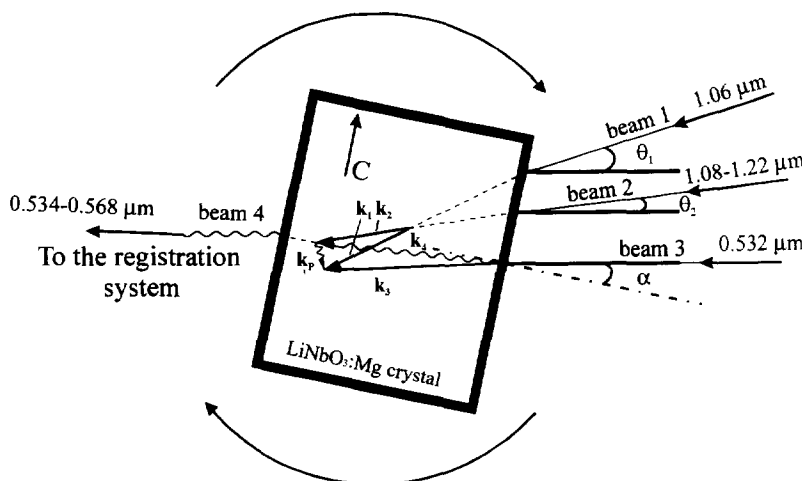


Fig. 1. Scattering geometry.

the direction of the signal of four-wave scattering coincides with the direction of the phase-matched three-wave spontaneous scattering, which is determined as

$$k_4^{\text{sp}} = k_3 - k_p.$$

The generation linewidths were approximately  $1 \text{ cm}^{-1}$  for the first and the second harmonics of the YAG:Nd<sup>3+</sup>-laser and  $6 \text{ cm}^{-1}$  for the LiF:F<sub>2</sub><sup>-</sup>-laser.

The general scheme of the experimental setup is shown in Fig. 2.

### 3. Tuning of the frequency and spatial phase matching

Exact satisfaction of the frequency relations (1), (3) and sufficiently small values of the phase mismatches  $\Delta k$  and  $\tau$  are necessary for the measurement of the polariton dispersion law  $\omega_p(k_p)$ . The temporal and spatial phase matching conditions were tuned in two stages.

At the first stage, for each value of the polariton frequency  $\omega_p$ , tunable laser frequency  $\omega_2$  and the frequency of the signal selection  $\omega_4$  were set up according to (1) and (3), respectively. Let us note that the double frequency selection (by the selective resonator of the tunable laser and by the spectral device in the registration channel) is not obligatory. In our case, it enabled us to eliminate additional parasite light at the input of the registration device. Measurements were carried out with different fixed values of the frequency difference  $\omega_1 - \omega_2 = \omega_p$ , both near the E-type phonon resonance ( $\omega_{\text{TO}} = 581 \text{ cm}^{-1}$ )

and at some distance from it. The spectral linewidth of the signal radiation  $\Delta\nu_4$  corresponded to the frequency structure of the three pumping beams. This value varied slightly when the angles of the exciting beams incidence were adjusted; sometimes it was smaller than the linewidth of the LiF:F<sub>2</sub><sup>-</sup>-laser  $\Delta\nu_2$ , but in all cases it did not exceed the sum of spectral linewidths of all pumping lasers.

At the second stage, tuning of spatial phase matching was carried out. This process seems to be the most complicated part of the experiment. In the case of scattering in the principal plane of the crystal there are three tuning parameters, the final precise tuning being done by any two of them. These three parameters are the angles determining mutual orientation of the three pumping beams and the principal axis of the crystal. We used an extraordinarily polarized probe beam with wavelength  $\lambda_L = 0.532 \mu\text{m}$  and exciting beam with  $\lambda_1 = 1.064 \mu\text{m}$ , the radiation of the tunable laser had ordinary polarization. Tuning of the spatial phase matching for the direct process can be done by varying any single parameter since condition (2) is not critical for it. It makes the observation of the direct process more convenient; however, in this case one cannot measure the parameters of the polariton wavevector.

We obtained lineshape curves of the four-wave scattering in the  $k$ -space. The sequence of operations was the following: the constant frequency difference  $\omega_1 - \omega_2 = \omega_p$  was set up; IR exciting beams were directed into the crystal at fixed angles  $\theta_1$  and  $\theta_2$  to the probe beam. We registered the scattered radiation intensity as a function of

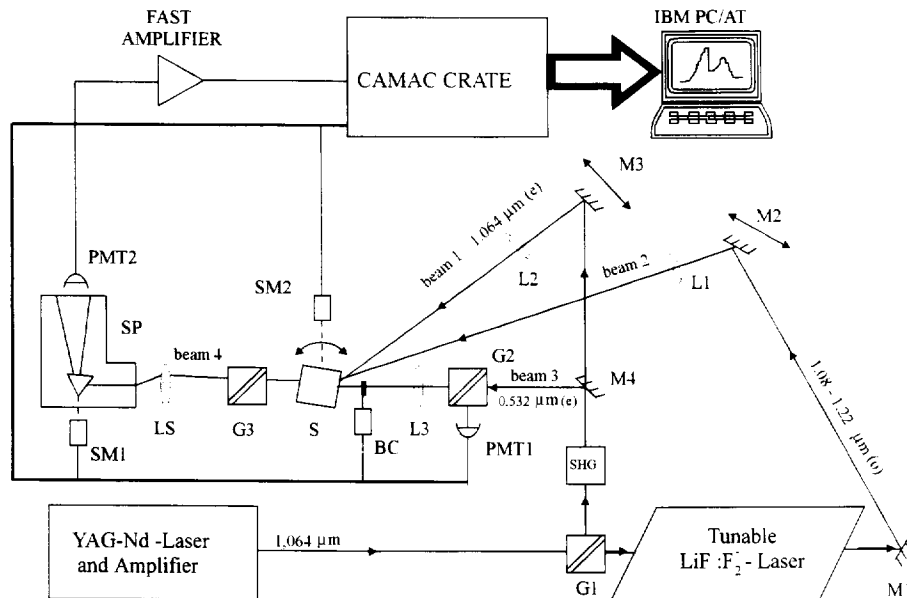


Fig. 2. Experimental setup. G1–G3 – Glan-Thompson polarizing prisms, L1–L3 – focusing lenses, LS – three-lens system, M1–M3 – mirrors, M4 – frequency selective mirror, SP – spectrometer, SHG – second harmonic generator, S – the studied sample. BC – beam chopper, SM1–SM2 – step motors, PMT1 – photomultiplier measuring the probe pump intensity, PMT2 – photomultiplier measuring the signal radiation intensity.

the angle of crystal rotation  $\alpha$  in the plane containing wavevectors of the pumping beams. The angles  $\alpha$ ,  $\theta_1$  and  $\theta_2$  were varied near their mean values, which were calculated from Eqs. (1)–(4) taking into account the dispersion of the crystal refractive index. For each fixed value of the signal frequency (or for the corresponding value of the polariton frequency) the exact phase matching conditions for cascade coherent four-wave scattering were satisfied on a curve in the space of the angles  $\alpha$ ,  $\theta_1$  and  $\theta_2$ . Assuming some phase mismatch, we find the scattering to occur in a limited area located around this curve. A series of line-shape measurements was performed for each value of the frequency difference  $\omega_1 - \omega_2 = \omega_p$ . In each series, we fixed the angle between the probe beam and one of the two exciting beams. As to the second exciting beam, its orientation with respect to the probe beam was varied from run to run.

A typical scattering lineshape curve  $I_S(\alpha)$  is shown in Fig. 3a. It has a single maximum with angular width of about  $1^\circ$ . The intensity of the four-wave scattering signal is

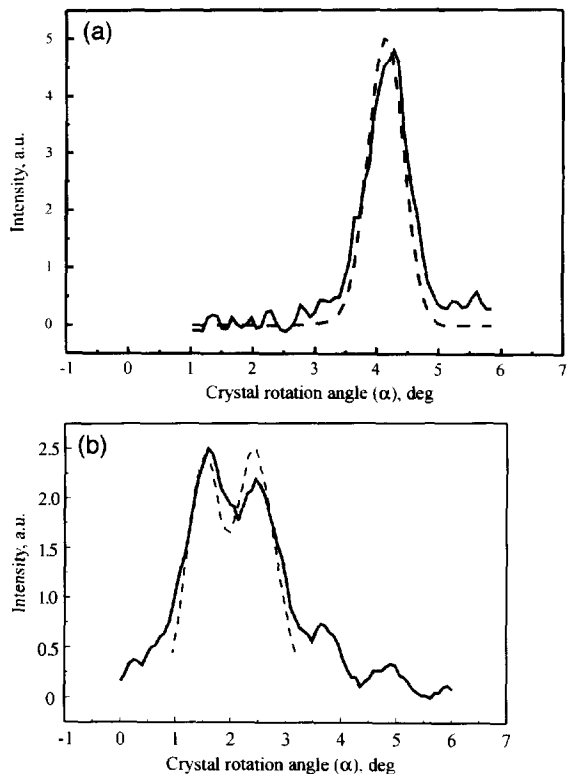


Fig. 3. Angular lineshapes of the four-wave scattering in LiNbO<sub>3</sub>:Mg crystal with Mg mass concentration of 0.68%. Solid curves – experiment, dashed curves – calculation. Polariton frequency is  $\omega_p = 558 \text{ cm}^{-1}$ . LiF:F<sub>2</sub><sup>-</sup>-laser beam's angle of incidence is  $\theta_2 = 19.2^\circ$  ( $\lambda_2 = 1.13 \text{ }\mu\text{m}$ ). Angles of incidence of the first exciting beam ( $\lambda_1 = 1.064 \text{ }\mu\text{m}$ ) are  $\theta_1 = 43.83^\circ$  (a) and  $\theta_1 = 43.27^\circ$  (b). Calculated parameters: polariton absorption  $\alpha_p = 24 \text{ cm}^{-1}$  (a),  $\alpha_p = 23 \text{ cm}^{-1}$  (b), effective interaction length  $L = 1.0 \text{ mm}$  (a) and  $L = 0.95 \text{ mm}$  (b).

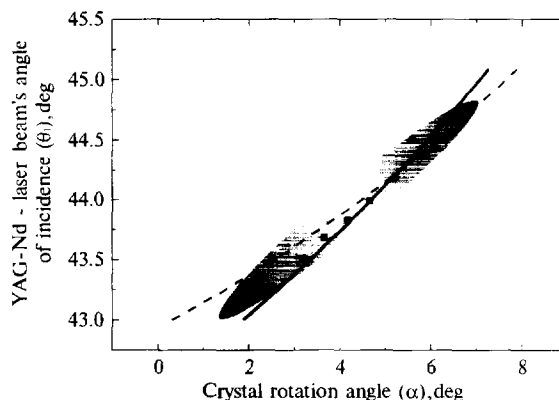


Fig. 4. Calculated spatial phase matching curves and positions of the experimental intensity maxima (squares). Solid curve –  $\Delta k = k_4 - k_3 + k_1 - k_2 = 0$ . Dashed curve –  $\vec{\tau} = \vec{k}_p - \vec{k}_1 + \vec{k}_2 = 0$ . The hatched area denotes the region where four-wave scattering is observed. The mass concentration of Mg is 0.68%. Polariton frequency is  $\omega_p = 558 \text{ cm}^{-1}$ . The angle of incidence of the LiF:F<sub>2</sub><sup>-</sup>-laser beam is constant –  $\theta_2 = 19.2^\circ$ .

sufficiently (approx. four orders) higher than the intensity of the three-wave spontaneous scattering of the probe beam. Note that the signal of the three-wave scattering did not need any exciting beams and was collected from the entire crystal length (1 cm). At the same time, the signal of the four-wave process was collected only from the region where the probe beam intersected the two exciting beams, its length being in the limits of 0.5–1 mm.

For certain values of the angles  $\theta_1$  and  $\theta_2$  we observed additional maxima. They had the same angular width and intensity of the same order as the primary maxima (e.g., see Fig. 3b). In order to analyze the general evolution of the intensity angular distribution for the signal radiation, it is more convenient to study a series of experimental lineshape curves  $I_S(\alpha)$ . In each series of the lineshape measurements, the distribution  $I_S(\alpha, \theta_i)$ , was registered under fixed angle  $\theta_2$  (or  $\theta_1$ ) and variable angle  $\theta_1$  ( $\theta_2$ ). Results for one of the series are shown in Fig. 4 on the plane  $\alpha$ – $\theta_1$ , where  $\alpha$  is the crystal rotation angle and  $\theta_1$  is the angle of incidence of the YAG:Nd<sup>3+</sup>-laser beam, the angle of incidence  $\theta_2$  and the frequency  $\omega_2$  being constant. The squares denote the positions of intensity maxima, observed both in the lineshapes  $I_S(\alpha)$  with a single peak and in the curves  $I_S(\alpha)$  with multiple ones. The hatched ellipse denotes the area where four-wave scattering is observed. Outside this area, the intensity of the signal radiation is negligibly small and has the same order as the signal of three-wave scattering of the probe wave. In fact, the hatched area is the cross-section of the region in the space of parameters  $\alpha$ ,  $\theta_1$  and  $\theta_2$ , in which the scattered radiation intensity  $I_S \neq 0$ , by the plane  $\theta_2 = \text{const}$ .

Let us turn to the analysis of the scattering theory in order to solve the problem of measuring the real and imaginary parts of the polariton wavevector (with their

help, one can obtain the values of the refractive index, absorption coefficient and complex dielectric function at the frequency of the polariton state).

**4. Analysis of the angular lineshape of scattering**

Among several works dedicated to the features of four-wave mixing processes in a noncentrosymmetric medium [5,8–12], the most detailed study of scattering lineshapes is given in Ref. [11]. Conditions of our experiment correspond to the case of weak intensities of the pumping beams and high absorption at the polariton frequency. Then, as it is shown in Ref. [11], the frequency-angular scattering lineshape is given by the following expression for the intensity of the scattered radiation  $I_S$ :

$$I_S \sim \text{sinc}^2\left(\frac{\Delta kL}{2}\right) \left[ \beta^2 + \frac{4\tau\beta}{\alpha_p^2 + 4\tau^2} + \frac{1}{\alpha_p^2 + 4\tau^2} \right]. \quad (5)$$

Here  $\tau$  is the value of the phase mismatch at the first stage of the cascade process (“heating” of the polariton state),  $\Delta k$  is the value of the phase mismatch of the direct four-wave process,  $L$  is the effective interaction length,  $\alpha_p$  is the absorption at the polariton frequency  $\omega_p$ ,  $\text{sinc}(x) = \sin x/x$ . Parameter  $\beta$  is given by the relation between the contributions of the direct and cascade processes to the scattering intensity:

$$\beta = \frac{n_p \cos \vartheta_p c}{4\pi\omega_p} \frac{\chi^{(3)}}{\chi_1^{(2)}\chi_2^{(2)}}. \quad (6)$$

Here  $\vartheta_p$  is the angle determining the polariton wavevector orientation in the crystal,  $\chi^{(3)}$  is the effective value of cubic nonlinear susceptibility (the corresponding contribution to nonlinear polarization is  $P_4^{(3)} = \chi^{(3)}E_1^*E_2E_3$ ,  $E_i$  are the amplitudes of the electric fields with frequencies  $\omega_i$ ),  $\chi_1^{(2)}$  and  $\chi_2^{(2)}$  are effective values of the quadratic nonlinear susceptibility determining the efficiencies of the first (when the polarization  $P_p^{(2)} = \chi_1^{(2)}E_1E_2^*$  occurs at frequency  $\omega_p$ ) and the second (when the polarization  $P_4^{(2)} = \chi_2^{(2)}E_3E_p^*$  occurs at frequency  $\omega_4$ ) stages of the cascade process, respectively. In our case, when all frequencies of pumping and signal waves are different, and for their chosen polarizations, the effective values of the susceptibilities are equal to

$$\begin{aligned} \chi^{(3)} &= 3\chi_{xxxx}^{(3)}(-\omega_4, -\omega_1, \omega_2, \omega_3) \cos\vartheta_{1z} \cos\vartheta_{3z}, \\ \chi_1^{(2)} &= \chi_{xxz}^{(2)}(-\omega_p, \omega_1, -\omega_2) \cos\vartheta_{1z} \\ &\quad + \chi_{xxy}^{(2)}(-\omega_p, \omega_1, -\omega_2) \sin\vartheta_{1z}, \\ \chi_2^{(2)} &= \chi_{xxz}^{(2)}(-\omega_4, \omega_3, -\omega_p) \cos\vartheta_{3z} \\ &\quad + \chi_{xxy}^{(2)}(-\omega_4, \omega_3, -\omega_p) \sin\vartheta_{3z}, \end{aligned}$$

where  $\vartheta_{iz}$  is the angle between the crystal Z-axis and the direction of the extraordinarily polarized electric field  $E_i$  (here  $i = 1, 3$ ).

The first term in brackets in (5) describes the four-wave

scattering determined by  $\chi^{(3)}$ . Its intensity is maximal everywhere where  $\Delta k = 0$ . The curve corresponding to such condition is shown in Fig. 4 as the dependence between the angle of incidence,  $\theta_1$ , and the angle of rotation of the crystal,  $\alpha$ . Eq. (5) enables one to interpret the general situation of scattering under tuning along the phase matching curve  $\Delta k = 0$ . The intensity of the scattered radiation is constant at large mismatches of the cascade process  $\tau^2 \gg \alpha_p^2/4$ , its value being determined by the cubic nonlinear susceptibility  $\chi^{(3)}$ . The contribution of the cascade process increases against the background of the direct one while getting close to the region where  $\tau \approx 0$ . The second term in brackets in (5) describes the interference between direct and cascade processes. Even if direct scattering is not observed since the value of  $\chi^{(3)}$  is negligibly small, the mutual influence of these processes can lead to a sufficient distortion of the scattering lineshape. The cascade process by itself is described by the third term in brackets in (5). The pure cascade process has a lineshape described by  $\text{sinc}^2(\Delta kL/2)$  multiplied by the Lorentzian factor  $1/(\alpha_p^2 + 4\tau^2)$ . The region where the cascade process can be observed (see Fig. 4) has to be located near the intersection of the curves corresponding to the conditions  $\Delta k = 0$  (solid curve) and  $\tau = 0$  (dashed curve). The dimensions of this region depend on the interaction length  $L$  (i.e., the width of the principal maximum of the function  $\text{sinc}^2(\Delta kL/2)$ ), the absorption at the polariton frequency  $\alpha_p$  (i.e., the width of the Lorentzian factor  $1/(\alpha_p^2 + 4\tau^2)$ ) and the divergences of the pumping beams. We detected neither immediate contribution of the direct four-wave process to the intensity of the scattered radiation nor interference structure connected with the second term in brackets in (5). It indicates that the effective components of cubic nonlinear susceptibility are relatively small. We estimate  $\beta\alpha_p < 10^{-2}$ , which corresponds to the ratio  $\chi^{(3)}\alpha_p/\chi_1^{(2)}\chi_2^{(2)} < 10^3 \text{ cm}^{-1}$ .

Comparison of the experimental results with the theory indicates that here we deal with cascade coherent scattering. High single scattering maxima are observed near the intersection of zero mismatch curves for direct four-wave process ( $\Delta k = 0$ ) and polariton excitation process ( $\tau = 0$ ). While moving from the intersection point, the widths of the maxima increase, intensity decreases and double maxima appear near the boundaries of the observation region. Two examples of the observed spectra, shown in Fig. 3, demonstrate the  $I_S(\alpha)$  dependences in the two opposite cases. In Fig. 3a, the angles of incidence of the pumping waves corresponded to the case where the two phase-matching conditions,  $\Delta k = 0$  and  $\tau = 0$ , were simultaneously satisfied for the same crystal orientation  $\alpha$ . So we observed a single sharp peak, located at this value of  $\alpha$ . In the case of Fig. 3b, the phase-matching conditions  $\Delta k = 0$  and  $\tau = 0$  were satisfied at two different values of  $\alpha$ . So the  $I_S(\alpha)$  dependence has two maxima. One of them is situated near the zero mismatch point  $\tau = 0$ , and the other one near the point  $\Delta k = 0$ . Scattering disappears if the

phase matching curves are displaced from one another by a distance larger than the sum width of the two maxima. Assuming pure cascade type of scattering, we calculated the interaction parameters, giving the best fit of the experimental results by (5) under the condition  $\beta = 0$ . We varied the value of the polariton absorption  $\alpha_p$ , effective interaction length  $L$ , and the effective diameter of the beams at the focusing lenses  $d$ . (The diameters of all beams were equal. Together with the focal lengths of the lenses, they determined the angular divergence of the beams.) Almost identical values of  $\alpha_p$ ,  $L$  and  $d$  were obtained for each spectrum registered at the signal frequency corresponding to the polariton frequency of  $558 \text{ cm}^{-1}$ :  $\alpha_p = 23 \pm 2 \text{ cm}^{-1}$ ,  $d = 1.25 \text{ mm}$ ,  $L = 0.8\text{--}1.0 \text{ mm}$ .

These values conform perfectly with the optical scheme of the experimental setup. The value of  $L$  could vary from spectrum to spectrum because the overlap of the beams in the crystal was not identical. The fact of quite perfect constancy of the adjusted parameters can be treated as an evidence of the chosen theoretical model correctness. However, the calculated values of polariton absorption  $\alpha_p$  disagree with the data obtained by other methods. Results of three-photon and IR-reflection [15] spectroscopy differ from the obtained value of  $\alpha_p$  by more than an order of magnitude. Calculation of the polariton absorption on the basis of the multiple oscillator model, using the data on the phonon oscillator strengths and phonon damping constants in  $\text{LiNbO}_3$  determined from Raman spectra [15], gives a value of  $\alpha_p$  of about  $5 \times 10^3 \text{ cm}^{-1}$  in the investigated frequency range. Differences between the true values of absorption in Mg-doped crystal and pure crystals of different stoichiometry compositions seem to be not so large as the discrepancy observed in our experiments. All other data on  $\text{LiNbO}_3$  polariton absorption in the considered spectral region sufficiently exceed the value obtained by the four-wave mixing method described above. There are no reasons to doubt their correctness. Next, note that the method of  $\alpha_p$  evaluation used previously for the bulk [5] and surface [16] polaritons in the GaP crystal, was based on the same interpretation of the four-wave scattering processes. The obtained values of polariton absorption at different frequencies were in rather better agreement with the ones obtained by other methods, calculated on the basis of the oscillator model. Though, in contrast to the polariton wavevector real part, they did not completely coincide with the results of IR reflectivity spectra or multiple-oscillator theory in the case of bulk polaritons and single-oscillator model in the case of surface polaritons. Each time they were smaller than that obtained by other methods. In our experiments, the discrepancy between the obtained values of  $\alpha_p$  and the same data of other methods is much larger. It makes us doubt about the chosen scattering model, though all other features of the observed phenomenon are perfectly described by it. Probably, in our case the parameter  $\alpha_p$  is determined not only by the imaginary part of the linear susceptibility, but depends also

on the power of the incident laser radiation through the nonlinear susceptibilities. We also see the opportunity to explain this phenomenon taking into account the weak photorefractive properties of  $\text{LiNbO}_3\text{:Mg}$ . However that may be, the possibility of measuring the polariton wave absorption is still doubtful.

## 5. Conclusion

Thus, the processes leading to four-photon light scattering were studied for  $\text{LiNbO}_3$  crystals with known values of polariton absorption and refractive index in the visible and IR ranges. From the viewpoint of further employment of this method, the following conclusions are significant:

(i) Considerable (approx. by 5 orders) amplification of the signal is achieved in comparison with the signal of spontaneous three-wave scattering in volumes of about  $1 \text{ mm}^3$ . It indicates that the size of the sample under study can be greatly reduced and one can study low-dimensional structures and inhomogeneities of polariton parameters distribution in macro-objects with high spatial resolution.

(ii) It is shown that the cascade type of scattering process is predominant in the frequency range of  $520\text{--}580 \text{ cm}^{-1}$  in the  $\text{LiNbO}_3$  crystal. It is this type of four-wave interaction process that is most sensitive to the state of the polariton parameters of a medium. The measurements performed show that the real part of the polariton wavevector can be determined with high precision. While analyzing the experimental results (Fig. 4), we used the value of the ordinary refractive index  $n_p = 6.270$ . This value improves the data obtained from the experiments on three-photon scattering. Its variation by only 0.005 leads to complete disagreement between calculated and observed data. At the same time, the accuracy of the spontaneous three-wave scattering method is several times lower.

(iii) The value of the polariton wavevector imaginary part, determined from the angular distribution of the scattered light intensity, disagrees with the data of other methods for  $\text{LiNbO}_3$  crystals.

The principal drawbacks of the four-wave mixing spectroscopy in comparison with the spontaneous three-wave polariton scattering are the following:

- the necessity to satisfy a large number of phase matching conditions. It leads to a more complicated way of the setup justification for the signal radiation disclosure;
- the possibility of the simultaneous registration of different types of scattering processes and their interference. It leads to difficulties in the primary interpretation of the experimental data;
- relative complexity of the experimental setup, which includes two or three laser sources, one of them being tunable;
- the possibility of measurement of the polariton wavevector imaginary part still remains unclear.

Nevertheless, four-wave mixing spectroscopy possesses the most important feature – essentially higher sensitivity.

Apparently, it is this advantage that will stimulate further evolution of the theory and research for constructing optimal spectroscopic schemes of cascade four-wave light scattering by polaritons.

### Acknowledgements

The authors are grateful to S.P. Kulik and M.V. Chekhova for useful remarks and the help in the preparation of the manuscript. The crystals of  $\text{LiNbO}_3:\text{Mg}$  were kindly supplied by Dr. I.I. Naumova from the Department of Crystal Physics of Moscow State University. This work was supported by the Russian Foundation of Basic Research (Grant No. 96-02-16336).

### References

- [1] A.S. Barker and R. Loudon, *Rev. Mod. Phys.* 44 (1972) 18.
- [2] Y.N. Polivanov, *Sov. Phys. Usp.* 21 (1978) 805.
- [3] D.N. Klyshko, *Photons and Non-linear Optics* (Gordon and Breach, 1987).
- [4] D.A. Kleinman, *Phys. Rev.* 174 (1968) 1027.
- [5] J.P. Coffinet and F. DeMartini, *Phys. Rev. Lett.* 22 (1969) 60.
- [6] F. Vallee and C. Flytzanis, *Phys. Rev. B* 46 (1992) 13799.
- [7] M.D. Levenson and N. Bloembergen, *Phys. Rev. B* 10 (1974) 4447.
- [8] E. Yablonovitch et al., *Phys. Rev. Lett.* 29 (1972) 865.
- [9] J.J. Wynne, *Phys. Rev. Lett.* 29 (1972) 650.
- [10] Yu.N. Polivanov and A.T. Sukhodolsky, *Sov. JETP Lett.* 25 (1977) 221.
- [11] V.L. Strizhevskii and Yu.N. Yashkir, *Sov. J. Quantum Electron.* 5 (1975) 541.
- [12] D.N. Klyshko, *Sov. J. Quantum Electron.* 5 (1975) 149.
- [13] A.L. Alexandrovskii et al., *Sov. J. Quantum Electron.* 21 (1991) 225.
- [14] D.S. Smith et al., *Optics Comm.* 17 (1976) 332.
- [15] A.S. Barker, Jr. and R. Loudon, *Phys. Rev.* 158 (1967) 433.
- [16] F. DeMartini et al., *Phys. Rev. Lett.* 37 (1976) 440.